THERMALLY STIMULATED CURRENT OBSERVATION OF TRAPPING CENTERS IN LAYERED THALLIUM DICHALCOGENIDE SEMICONDUCTORS

A THESIS SUBMITTED TO
THE GRADUATE SCHOOL OF NATURAL AND APPLIED SCIENCES
OF
MIDDLE EAST TECHNICAL UNIVERSITY

BY

NUH SADİ YÜKSEK

IN PARTIAL FULFILLMENT OF THE REQUIREMENTS

FOR

THE DEGREE OF MASTER OF SCIENCE

IN

PHYSICS

AUGUST 2004

Approval of the Graduate School of Natural and Applied Sciences.

Prof. Dr. Canan Özgen
Director

I certify that this thesis satisfies all the requirements as a thesis for the degree of Master of Science.

Prof. Dr. Sinan Bilikmen
Head of Department

This is to certify that we have read this thesis and that in our opinion it is fully adequate, in scope and quality, as a thesis for the degree of Master of Science.

Prof. Dr. Nizami Hasanli
Co-Supervisor

Prof. Dr. Hüsnü Özkan
Supervisor

Examining Committee Members

Prof. Dr. Yakup Cevdet Akgöz (METU, ES) _____

Prof. Dr. Hüsnü Özkan (METU, PHYS) _____

Prof. Dr. Nizami Hasanli (METU, PHYS) _____

Prof. Dr. Raşit Turan (METU, PHYS) _____

Prof. Dr. Cüneyt Can (METU, PHYS) _____

I hereby declare that all information in this document has been obtained and presented in accordance with academic rules and ethical conduct. I also declare that, as required by these rules and conduct, I have fully cited and referenced all material and results that are not original to this work.

Name, Last name : Nuh Sadi Yüksek

Signature :

ABSTRACT

THERMALLY STIMULATED CURRENT OBSERVATION OF TRAPPING CENTERS IN LAYERED THALLIUM DICHALCOGENIDE SEMICONDUCTORS

Yüksek, Nuh Sadi
M.S., Department of Physics
Supervisor: Prof. Dr. Hüsnü Özkan
Co-Supervisor: Prof. Dr. Nizami Hasanli

August 2004, 40 pages.

Thermally stimulated current measurements are carried out on as-grown $TlGaS_2$, $TlGaSe_2$ and $TlInS_2$ layered single crystals with the current flowing perpendicular to the *c*-axis in the wide temperature range of 10-300 K with various heating rates. Experimental evidence is found for the presence of three, two and one trapping centers for $TlGaS_2$, $TlGaSe_2$ and $TlInS_2$ crystals with activation energies 6, 12 and 26; 98 and 130; 12 meV respectively. We have determined the trap parameters using varous methods of analyis, and these agree well with each other.The retrapping process is negligible for these levels, as confirmed by good agreement between the experimental results and theoretical predictions of the model that assumes slow retrapping. Also the calculated values of the capture cross sections, attempt to escape frequencies and the concentration of the traps are reported.

Keywords: Layered semiconductors, Defects, Electrical properties

ÖZ

TALYUM İKİLİ ÇALKOGENİT KATMANLI YARIİLETKEN KRİSTALLERDE ISILUYARILMIŞ AKIMLARLA GÖZLENEN TUZAK SEVİYELERİ

Yüksek, Nuh Sadi
Yüksek Lisans, Fizik Bölümü
Tez Yöneticisi: Prof. Dr. Hüsnü Özkan
Ortak Tez Yöneticisi: Prof. Dr. Nizami Hasanli

Ağustos 2004, 40 sayfa.

Isıluyarılmış akım ölçümleri, katkılanmamış $TlGaS_2$, $TlGaSe_2$ ve $TlInS_2$ kristallerinde c-exsenine dik olacak şekilde $10-300$ K geniş sıcaklık aralığında gerçekleştirildi. Deney sonuçları $TlGaS_2$, $TlGaSe_2$ ve $TlInS_2$ kristalleri için enerjileri sırasıyla 6, 12 ve 26; 98 ve 130; 12 meV olan 3, 2 ve 1 tuzak seviyesi olduğunu gösterdi. Yapılan hesaplamalarda yavaş tuzaklanma varsayımı yapılmış olup hesaplanan yakalama kesit alanı, kaçış frekansı ve tuzak yoğunluğu parametrelerinin değerleri de bu çalışmada sunulmuştur.

Anahtar Sözcükler: Katmanlı yarıiletkenler, Safsızlıklar, Elektriksel Özellikler

ACKNOWLEDGMENTS

Many great thanks are due to my family for their continuous support and understanding.

Nor I can forget what I owe to Prof. Dr. Hüsnü Özkan who has made countless productive and useful suggestions in every part of this work, which has greatly benefited from his careful reading and critical comments.

I would like to express my deepest gratitude to my co-advisor Prof. Dr. Nizami Hasanli. Without his excellent supervision, encouragement, invaluable comments and helps, friendly attitude, patience and continuous support I would never have been able to undertake and carry out this work.

Finally, I am particularly indepted to my friends Hüseyin Kavas, Özgür Karci, Mustafa Fatih Genişel, Coşkun and Aşkın Kocabaş twins, Muhammed Açıkgöz, Ahmet Tombak, Feridun Ay and İsa Kiyat and also Assoc. Prof. Dr. Mustafa Göktepe for their encouragement, invaluable helps, patience and support.

TO BETÜLCÜK...

TABLE OF CONTENTS

LIST OF TABLES

LIST OF FIGURES

CHAPTER 1

INTRODUCTION

Recently, ternary thallium chalcogenides $TlGaS_2$, $TlGaSe_2$ and $TlInS_2$ received a great deal of attention due to their optical and electrical properties in view of possible optoelectronic device applications $[1-4]$. These III-III-VI_2 family of crystals have layered structures. At room temperature, layer-structured thallium chalcogenide crystals belong to the monoclinic system, and their space group is C2/c. The lattice of these crystals consists of alternating two-dimensional layers arranged parallel to the (001) plane. Each successive layer is rotated by a 90° angle with respect to the previous layer.

$TlGaS_2$ is a semiconductor with an indirect band gap of about 2.46 and 2.55 eV at 300 and 10 K, respectively [5]. A high sensitivity in the visible range of spectra, high birefrengence in conjunction with a wide transparency range of 0.5-14 μm, make this crystal useful for optoelectronic applications [6]. For possible applications in optoelectronic devices in the visible range, much attention has been devoted to the study of the optical and electrical properties of $TlGaS_2$ $[7-9]$. In this regard, detailed information on the impurity and defect centers is very useful for the fabrication of high-quality devices. The thermally stimulated currents (TSC) technique has been extensively used in the past to determine the thermal ionization properties of imperfection centers in semiconductors $[10-12]$.

Recently, the photoluminescence (PL) of $TlGaS_2$ single crystals [9], showed

broad emission bands, which is attributed to donor-acceptor pair recombination. Song et al. [8] have investigated the deep levels of $TlGaS_2$ crystals in the temperature range $90-350$ K by TSC and photoinduced current transient spectroscopy techniques. The activation energies of the observed four peaks were found to be 180, 230, 360 and 660 meV. However, there has yet been no study on the shallow levels of $TlGaS_2$ single crystals in the temperature range below 90 K.

$TlGaSe_2$ crystal has direct band gap energy of 2.19 and 2.11 eV at 10 and 300 K, respectively [1]. A high photosensitivity in the visible range of spectra, high birefringence in conjunction with a wide transparency range of 0.5-14 μm make $TlGaSe_2$ crystal useful for optoelectronics applications [6]. In this regard, detailed information on the presence of the impurity and defect centers in the crystal is important to fabricate high-quality devices. In the past, Raman, Brillouin and infrared spectra [13 – 15], optical and dielectric properties [16], exciton spectra and phase transition [17, 18], and absorption spectra [19] of the $TlGaSe_2$ crystals have been studied. Bakhyshov *et al.* [20] have investigated the deep levels of $TlGaSe_2$ crystals in the temperature range $100-300$ K by TSC spectroscopy technique. The activation energies of the observed three peaks were found to be 370, 600 and 680 meV. Only activation energies of the traps were determined with initial rise method. Other methods have not been applied to TSC spectra of $TlGaSe_2$ crystal to obtain the activation energy and other parameters of the trapping centers.

Among many $TlBX_2$-type compounds, $TlInS_2$ has been studied rather well. The forbidden gap of $TlInS_2$ was measured by both absorption and reflection

spectroscopy as a function of temperature and was found to be a direct band gap with an energy of 2.58 eV at $T = 10$ K [21, 22]. A high photosensitivity in the visible range of spectra, high birefringence in conjunction with a wide transparency range of 0.5-14 μm make this crystal useful for optoelectronic applications [6]. For possible applications in optoelectronic device in the visible range, a great deal of attention has been devoted to the study of the structural [4, 23, 24], electrical [1, 25, 26] and optical [6, 21, 22, 25, 27, 28] properties. In this regard, detailed information on the presence of the impurity and defect centers in the crystal is very useful to fabricate high-quality devices. The thermally stimulated currents (TSC) technique has been extensively used in the past to determine the thermal ionization properties of imperfection centers in semiconductors $[10 - 12]$.

In Ref. [29], the temperature dependencies $(11 - 100$ K) of the PL spectra in $TlInS_2$ crystal have been presented. Two PL bands were observed centered at 515 nm (2.41 eV, A-band) and 816 nm (1.52 eV, B-band) at $T = 11$ K. Analysis of the data showed that the A-band was due to radiative transitions from the moderately deep donor level located at 250 meV below the bottom of the conduction band to the shallow acceptor level located at 20 meV above the top of the valence band. There is only one paper in literature concerning the study of TSC spectra in $TlInS_2$ crystals in the high-temperature range $90 - 300$ K [30]. A series of trap levels with energy depths ranging from 150 to 220 meV has been found in the energy gap. However, the shallow levels in $TlInS_2$ crystal in the temperature range below 90 K have not been studied.

The purpose of the present work is to obtain detailed information concerning shallow traps in undoped $TlGaS_2$, $TlGaSe_2$ and $TlInS_2$ layered crystals using the well-established technique of TSC measurements. In contrast with previous TSC measurement on $TlGaS_2$ and $TlInS_2$, we for the first time employ a low temperature range of $10 - 90$ K. This temperature range allows us to check for the possibility of extremely shallow trap states. On $TlGaSe_2$ we employed, for the first time, the wide temperature range of 10-300 K. We used various methods to analyze the measured TSC spectra. The activation energy, the capture cross section, attempt to escape frequency and concentration of the traps in $TlGaS_2$, $TlGaSe_2$ and $TlInS_2$ crystals are reported.

CHAPTER 2

THEORY OF THERMALLY STIMULATED CURRENT

2.1 Introduction

When a semiconductor or insulator is heated, after a band-gap excitation at low temperature, the transient enhancement of electrical conductivity (thermally stimulated current or TSC) can be measured. The characteristics of the resulting TSC are dictated by the properties of shallow and deep levels within the band-gap.

A donor is an impurity which gives rise to an energy level within the band-gap and is neutral at zero Kelvin. As the temperature increases the donor becomes ionized thus 'donating' an electron to the conduction band. As the temperature is again lowered the ionized donor reclaims an electron from the conduction band and returns to its neutral state. Although, at lower temperatures, the donor captures an electron, it is not considered a trap since it is simply reclaiming what it donated earlier. An electron trap, on the other hand, does not have excess electrons to donate to the conduction band at high temperatures. Traps do, however, capture electrons from the conduction band at lower temperatures possibly removing the electrons which were thermally excited from shallow donors (i.e. compensation).

An electron recombination center is often referred to as a hole trap. This defect level contains trapped holes which act as recombination sites for electrons

in the conduction band. At higher temperatures there may be sufficient thermal energy to excite these holes to the valence band. The excitation of carriers out of a defect is indicative of trap like behavior. In conclusion, if the probability of recombination is much greater than the probability of thermal excitation then the center is a recombination center. However if the probability of excitation is greater then the center is a trap. From this argument, it may be summarized that a given defect may act as a trap at high temperatures and as a recombination center at low temperatures

2.2 Development of Theory

In order to describe the kinetics of TSC, possible transitions shown in Fig. 2.1 must be described. Since we are only considering the capture of electrons (transitions 1 and 2) by the electron traps of concentration N_t and capture cross

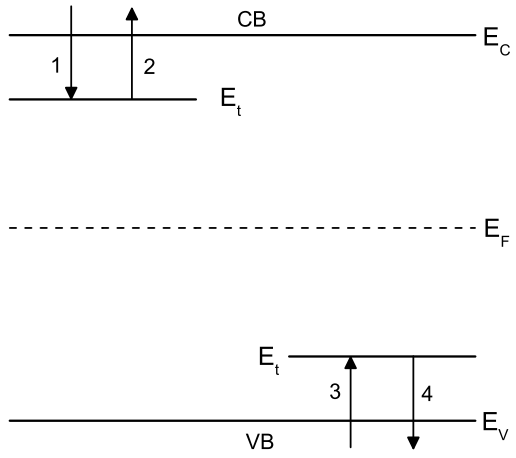

Figure 2.1: Energy Band diagram of a single level system

sections S_t, it is easier to imagine that the traps are moving through the sample in which electrons are stationary [31]. Assume that the concentration of previously

filled traps in n and that the traps are moving at a velocity υ_e (thermal velocity of electrons in the conduction band). While the $(N-n)$ empty traps are travelling through the sample they scan a fractional volume per unit time of $(N-n)S_t\upsilon_e$. Therefore, the rate of electron capture in $n_c(N-n)S_t\upsilon_e$ where n_c is the free electron concentration.

The thermal excitation of an electron from a trap of depth E_t below the conduction band (transition 2) is characterized by the attempt to escape frequency ν and the probability of thermal excitation $\exp(-E_t/kT)$ where k is the Boltzmann's constant. The pruduct of these two terms gives the probability per unit time of an electron being thermally excited to the conduction band. Then the rate of excitation is given as $n\nu\exp(-E_t/kT)$.

The expression for the rates of trapping and detrapping may be combined to give the time rate of change of trapped electrons, namely

$$\frac{dn}{dt} = n_c(N-n)S_t\upsilon_e - n\nu\exp\left(-\frac{E_t}{kT}\right) \tag{2.1}$$

The quantity ν, referred to as the frequency factor, or attempt to escape frequency, may be written as

$$\nu = N_c S_t \upsilon_e \tag{2.2}$$

Where N_c is the effective density of states in the conduction band. N_c and υ_e are given by:

$$N_c(T) = 2\left(\frac{kTm_e^*}{2\pi\hbar^2}\right)^{2/3} \tag{2.3}$$

and

$$\upsilon_e(T) = \sqrt{\frac{3kT}{m_e^*}} \tag{2.4}$$

where m_e^* is the electron effective mass in the conduction band.

It is usually assumed that the frequency factor ν follows a power law temperature dependence [32], that is,

$$\nu(T) = BT^{2-b} \tag{2.5}$$

where B and b are constants and $0 \leq b \leq 4$. By combining equations 2.2, 2.3 and 2.5 it is found that the capture cross section also follows a power law temperature dependence defined as

$$S_t(T) = \frac{B(2\pi\hbar^2)^{3/2}}{2\sqrt{3}m^*k^2}T^{-b} = CT^{-b} \tag{2.6}$$

where C is a parameter dependent upon the effective mass.

There are two paths through which charge may be added to or removed from the conduction band: (1) The trap level is capable of both adding and removing charge. Any charge added to (removed from) the trap level is removed from (added to) the conduction band; (2) The recombination path removes charge from the conduction band through the recombination of an electron and a trapped hole. The rate of this recombination is n_c/τ where τ is the recombination lifetime [31].

The rate equations describing the rate of change of free and trapped charge may be written as:

$$\frac{dn}{dt} = n_c(N-n)S_t\upsilon_e - nN_cS_t\upsilon_e \exp\left(-\frac{E_t}{kT}\right) \tag{2.7}$$

and

$$\frac{dn_c}{dt} = -\frac{dn}{dt} - \frac{n_c}{\tau} \tag{2.8}$$

where the temperature dependencies of S_t, υ_e and N_c are implicit.

The solution of equations 2.7 and 2.8 usually proceeds from two fundamental assumptions which were first introduced by Randall and Wilkins [33]. The assumptions are: (1) the rate of retrapping of charge that has been released from a trap is negligible compared to the rate of recombination (i.e. first order kinetics), and (2) the system is close to equilibrium. That is, the rate of change of free electrons is small compared to the detrapping and recombination rates (i.e. Quasi-Equilibrium or QE). These assumptions may be expressed as

$$\frac{n_c}{\tau} \gg n_c(N-n)S_t\upsilon_e \tag{2.9}$$

and

$$\left|\frac{dn_c}{dt}\right| \ll \left|\frac{dn}{dt}\right| \tag{2.10}$$

respectively.

Applying these approximations to Eqs. 2.7 and 2.8 leads to

$$\frac{dn}{dt} \approx -n\nu \exp\left(-\frac{E_t}{kT}\right) \tag{2.11}$$

and

$$\frac{dn}{dt} \approx -\frac{n_c}{\tau} \tag{2.12}$$

Integration of Eq. 2.11, using the relationship $T = T_o + \beta t$, results in

$$n = n_o \exp\left\{-\int_{T_o}^{T} \frac{\nu}{\beta} \exp\left(-\frac{E_t}{kT}\right) dT\right\} \tag{2.13}$$

Where n_o is the initial trapped electron concentration and T is temperature.

Substituting Eqs. 2.12 and 2.13 into Eq. 2.11 leads to

$$n_c = n_o\tau\nu \exp\left\{-\frac{E_t}{kT} - \int_{T_o}^{T} \frac{\nu}{\beta} \exp\left(-\frac{E_t}{kT}\right) dT\right\} \tag{2.14}$$

$$\sigma = n_c e\mu = n_o \tau e \mu \nu \exp\left\{-\frac{E_t}{kT} - \int_{T_o}^{T} \frac{\nu}{\beta} \exp\left(-\frac{E_t}{kT}\right) dT\right\} \tag{2.15}$$

Here, σ is the thermally stimulated conductivity, n_o is the initial density of filled traps, τ is the lifetime of a free electron, μ is the electron mobility, β is the heating rate, T_o is the temperature at which heating begins, following the filling of the traps, ν is the attempt-to-escape frequency of a trapped electron, and k is the Boltzmann constant.

2.3 Curve Fitting Method

If we assume ν to be independent of T and ignore the variation of μ and τ with T over the temperature span of TSC curve, Eq. 2.15 can be rewritten as

$$\sigma = A \exp\left\{-t + B \int_{t_o}^{t} \exp(-t) t^{-2} dt\right\} \tag{2.16}$$

where $t = E_t/kT$ and A and B are constants:

$$A = n_o \tau e \mu \nu \qquad\qquad B = \nu E_t / \beta k \tag{2.17}$$

Repeated integration by parts of the integral in Eq. 2.16 leads to a convergent series, and then

$$\sigma = A \exp\left[-t - B\left\{\exp(-t)t^{-2} - 2\exp(-t)t^{-3} + 3 \times 2 \exp(-t)t^{-4} ...\right\}_{t_o}^{t}\right] \tag{2.18}$$

An approximate value of σ can be obtained by dropping all but the first term in the series

$$\sigma \simeq A \exp\{-t - B \exp(-t) t^{-2} |\, {}_{t_o}^{t}\} \tag{2.19}$$

$$\sigma \simeq \sigma_o + A \exp\{-t - B \exp(-t) t^{-2}\} \tag{2.20}$$

where σ_o is the value of σ at t_o. If Eq. 2.21 is differentiated and equated to zero to find the maximum of the curve, which occurs at $t = t_m = E_t/kT_m$, then

$$B = \exp(t_m)\frac{t_m^3}{t_m + 2} \tag{2.21}$$

In TSC spectra of a sample, if more than one peaks were observed, T_1, T_2... and T_n, overlapping each other, the fitting function comprising the sum of all features of the TSC peak spectrum was built as;

$$\sigma(T) = \sum_{i=1}^{m} \sigma_i(T) \tag{2.22}$$

where $\sigma_i(T)$ denotes contribution of each peak alone, calculated by means of Eq. 2.20, and m denotes number of traps involved in the calculation. Once the curve have been fitted and the values of E_t and T_m for each peak are determined, Eqs. 2.21 and 2.17 can be used to calculate B and the attempt-to-escape frequency ν, respectively. Knowing the value of ν, one can calculate the capture cross section of the traps according to following expression

$$S_t = \frac{\nu}{N_c \upsilon_e} \tag{2.23}$$

where N_c is the effective density of states in the conduction band and υ_e is the thermal velocity of a free electron.

The concentration of the traps was estimated using the relation [40]

$$N_t = \frac{Q}{ALGe} \tag{2.24}$$

Here, Q is the quantity of charge released during a TSC experiment and can be calculated from the area under the TSC peaks; A and L are the area and the thickness of the sample, respectively; e is the electronic charge and G is the

photoconductivity gain, which equals to the number of electrons passing through the sample for each absorbed photon. N_t was calculated by assuming $G = 1$, because it was not possible to measure G under the same TSC conditions with the necessary accuracy.

2.4 Peak Shape Method

In the peak shape method [37], the activation can be evaluated by using three parameters: $\tau = T_m - T_l,\ \delta = T_h - T_m,\ \omega = T_h - T_l$, where T_m is the temperature corresponding to the maximum current, T_l and T_h are the low and high half-intensity temperatures, respectively. The activation energy of the trap is then

$$E_\tau = \left\{ \frac{[1.51 + 3.0(\mu_g - 0.42)]\, kT_m^2}{\tau} \right\} - [1.58 + 4.2\ (\mu_g - 0.42)]\, 2kT_m \tag{2.25}$$

$$E_\delta = \frac{[0.976 + 7.3\ (\mu_g - 0.42)]\, kT_m^2}{\delta} \tag{2.26}$$

$$E_\omega = \left\{ \frac{[2.52 + 10.2\ (\mu_g - 0.42)]\, kT_m^2}{\omega} \right\} - 2kT_m \tag{2.27}$$

Here $\mu_g = \delta/\omega$, the value of which is predicted by Chen and Kirsh [37] as 0.42 for first order and 0.52 for second order kinetics. Since the peak shape method is not heating rate dependent the values of μ_g and energy values are calculated for different rates.

2.5 Initial Rise Method

The observation that the initial rise portion of a TSC curve may be described by a simple exponential was first made by Garlick and Gibson [38]. They applied

the approximation that $n \approx n_o$ for $T \approx T_o$ where T_o is a low enough temperature that the trap is not very active. As a general rule, the value of T_o should correspond to a temperature for which the magnitude of the TSC does not exceed 15 percent of the peak maximum. By describing TSC by the relation

$$I = C \times \exp\left(-\frac{E_t}{kT}\right) \tag{2.28}$$

where C is constant and I represents TSC; the activation energy is obtained from a line of slope $-E_t/k$ on a plot of $\ln(I)$ versus $1/T$.

In order to apply the initial rise technique, there must be no overlap in the initial rise portion of the peak under study.

2.6 Heating Rate Method

The relation of the heating rate with peak temperature is expressed as [37]

$$\beta = \nu \frac{kT_m^2}{E_t} \exp\left(-\frac{E_t}{kT_m}\right) \tag{2.29}$$

If we assume the T dependence of ν as $\nu \propto T^\alpha$, then

$$\frac{1}{\beta} = C\frac{E_t}{k}\left(\frac{1}{T_m}\right)^{2+\alpha} \exp\left(\frac{E_t}{kT_m}\right) \tag{2.30}$$

where C is constant

If various heating rates are employed and T_m are determined as a function of β , it is possible to derive the parameters α and E_t from the theoretical fit using Eq. 2.30 to the experimental data of $1/\beta$ vs. T_m.

CHAPTER 3

EXPERIMENTAL PROCEDURES

3.1 Experimental Procedures and Apparatus

In a TSC experiment, the sample is cooled to low temperature and is illuminated with a light source which excites carriers across the band-gap. Some of these carriers become trapped (transitions 1 and 3 in Fig. 2.1) where they will remain until a sufficient amount of thermal energy is applied through heating to excite the trapped carriers to their respective delocalized band (transitions 2 and 4 in Fig. 2.1). This heating is normally performed on a linear time scale at a heating rate β (i.e. $T = T_o + \beta t$). When a sufficient amount of thermal energy is applied, the trapped electrons (or holes) are thermally excited to the delocalized band, transition 2 (4), where they contribute to the electrical current thus giving rise to TSC transients. Since the concentrations of the various defect levels are usually small (for example: $\sim 10^{12}$ to 10^{16} cm^{-3}) compared to carrier concentrations of high conductivity semiconductors (10^{18} to 10^{22} cm^{-3}), the associated TSC signals might be very weak; often on the order of a few picoamperes at fields strengths of a few volts per mm. Since the background currents in low resistivity semiconductors (at similar fields) are many orders of magnitude larger, it is not possible to measure TSC for these samples since the high carrier concentration causes a rapid depletion of recombination centers. Although not useful for low resistivity samples, TSC is very sensitive technique capable of detecting very low

defect concentrations.

$TlGaS_2$, $TlGaSe_2$ and $TlInS_2$ polycrystals were synthesized from high purity elements (at least 99.999 percent) taken in stoichiometric proportions. Single

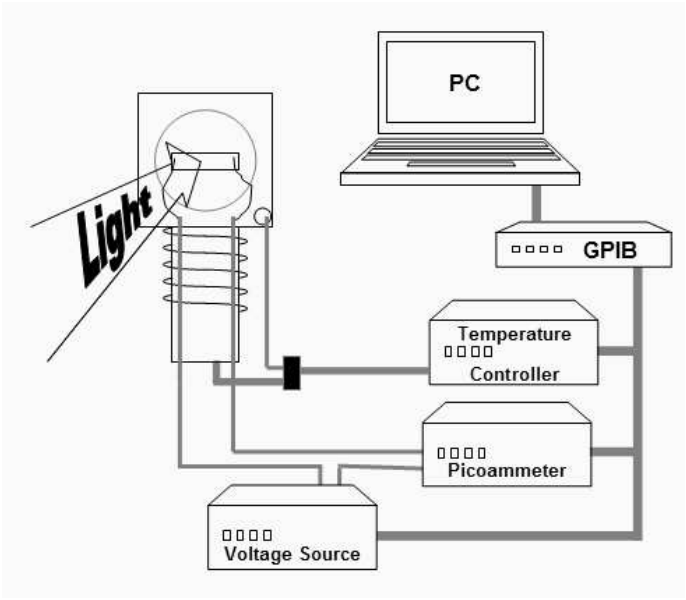

Figure 3.1: Schematic diagram of the sample on TSC experiment.

crystals were grown by the modified Bridgman method. No intentional doping of the crystals was performed. The X-ray diffraction patterns show that these crystals have monoclinic structure with the lattice parameters: $a = 1.031$, $b = 1.043$, $c = 1.507$ nm and $\beta = 99.60^\circ$ for $TlGaS_2$; $a = 1.076$, $b = 1.073$, $c = 1.560$ nm and $\beta = 99.92^\circ$ for $TlGaSe_2$ and $a = 1.094$, $b = 1.048$, $c = 1.561$ nm and $\beta = 100.70^\circ$ for $TlInS_2$. The samples were prepared by cleaving an ingot parallel to the crystal layer, which was perpendicular to the c-axis. The typical sample dimensions are $15 \times 5 \times 2$ mm^3 ($TlGaS_2$); $9 \times 4 \times 0.5$ mm^3 ($TlGaSe_2$); $8 \times 3 \times 0.5$ mm^3 ($TlInS_2$). The electrical conductivity of the studied samples was p-type as determined by the hot probe method.

To carry out TSC measurements, electrical contacts were made on the sample

surface with silver paste according to gap geometry (Fig. 3.1). In this configuration, the electrodes are placed at two opposite edges of the front surface of the crystal. The sample was mounted on the cold finger of the cryostat with a

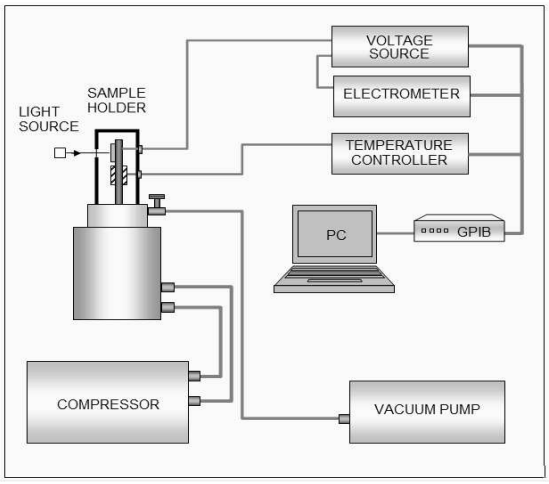

Figure 3.2: Schematic diagram of the TSC experimental setup.

non-conducting g-varnish. Thin copper wires were attached to the electrodes by small droplets of silver paste.

The TSC measurements have been performed from 9 to 300 K using an Advanced Research Systems closed-cycle helium gas cooling cryostat. Constant heating rates in the range of 3-60 K/min have been obtained by applying dc current to a 37.5 Ω NiCr heater filament wound around the sample holder. Linear increase of temperature has been achieved by a Lake-Shore 331 temperature controller utilizing the temperature sensor. Keithley 228A Voltage/Current source and Keithley 6485 picoammeter are used to measure TSC (Fig. 3.2). The temperature sensitivity of the system is about 10 mK and the current sensitivity of the TSC system is approximately 1 pA. At low enough temperatures, when the probability of thermal release is negligible, carriers are photo-excited using

a LED, generating light at a maximum peak of 2.6 eV, and trapped in the gap states. When the excitation is turned off and an expectation time has elapsed, the DC field is applied to the sample and the temperature is increased at a constant rate. The TSC is obtained from the current in excess of the equilibrium dark current contribution.

The details of time period of illumination, voltage, initial temperature details for $TlGaS_2$, $TlGaSe_2$ and $TlInS_2$ crystals are demonstrated in Figs. 3.3, 3.4 and 3.5, respectively

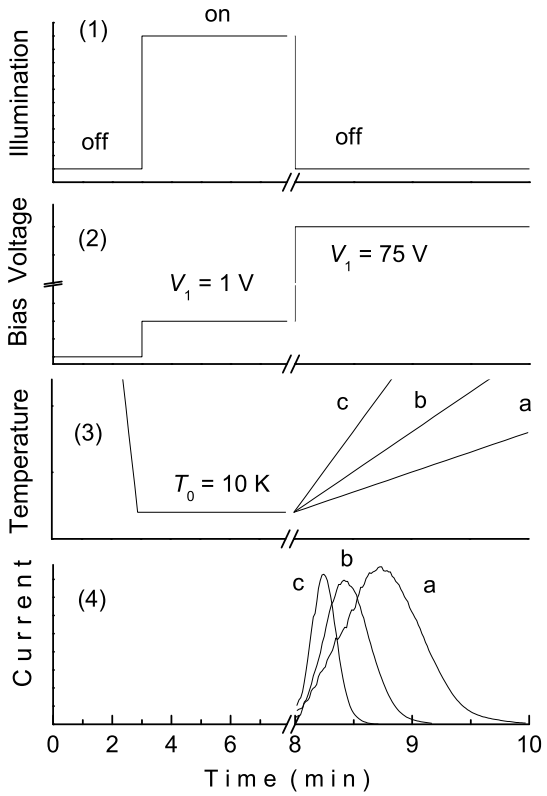

Figure 3.3: Principles of TSC experiment for $TlGaS_2$ crystals: (1) time period of applied illumination; (2) variation of bias voltage; (3) temperature variation with time; (4) TSC signal for three linear heating rates: 15 (a), 30 (b), 60 K/min (c).

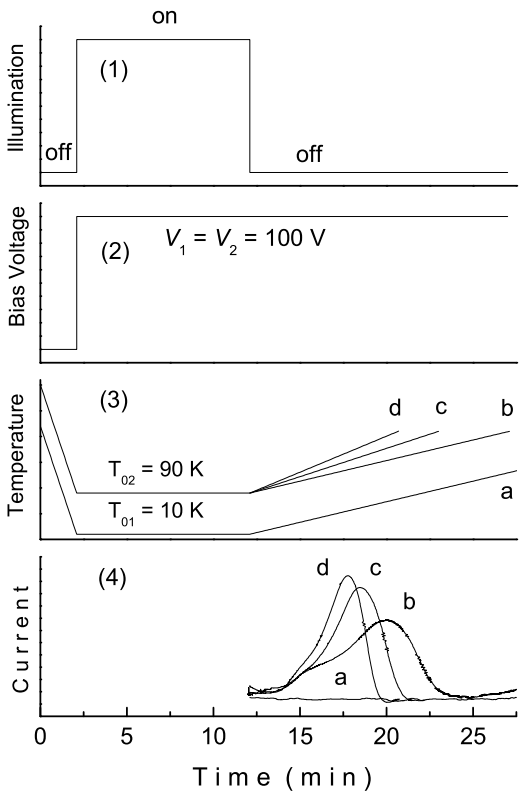

Figure 3.4: Principles of TSC experiment for $TlGaSe_2$ crystals: (1) time period of applied illumination; (2) variation of bias voltage; (3) temperature variation with time; (4) TSC signal for three linear heating rates: 8 (a), 8 (b), 11 (c), 14 K/min (d).

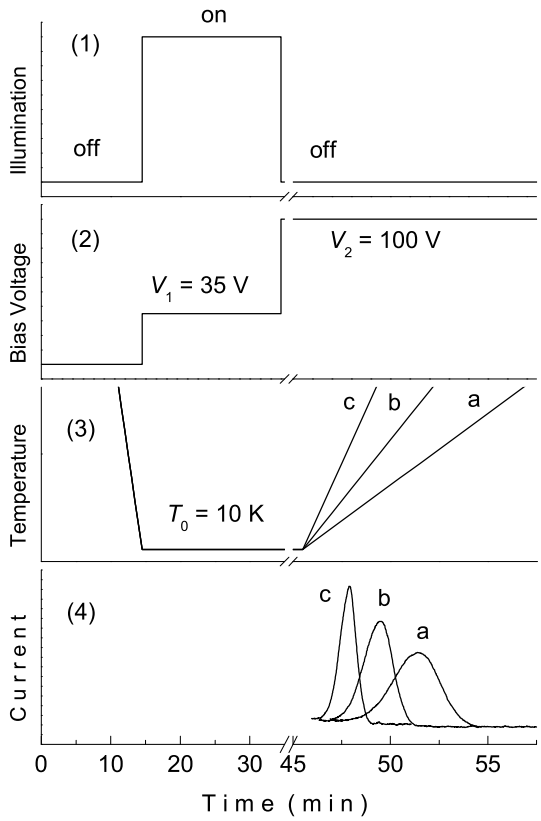

Figure 3.5: Principles of TSC experiment for $TlInS_2$ crystals: (1) time period of applied illumination; (2) variation of bias voltage; (3) temperature variation with time; (4) TSC signal for three linear heating rates: 6 (a), 10 (b),18 K/min (c).

CHAPTER 4

RESULTS AND DISCUSSION

4.1 Introduction

In this part of the thesis, we deal with the details of TSC experiments for each of the three layered ternary crystals ($TlGaS_2$, $TlGaSe_2$, $TlInS_2$). We will also give some results for each.

4.2 Results and Discussion of the TSC Experiment of $TlGaS_2$

Figure 4.1 shows the typical TSC spectra of $TlGaS_2$ single crystals for different heating rates of $\beta = 15$, 30, and 60 K/min in the 10-55 K temperature range [36]. The TSC curves are shifted, as expected, to high temperature with increasing the

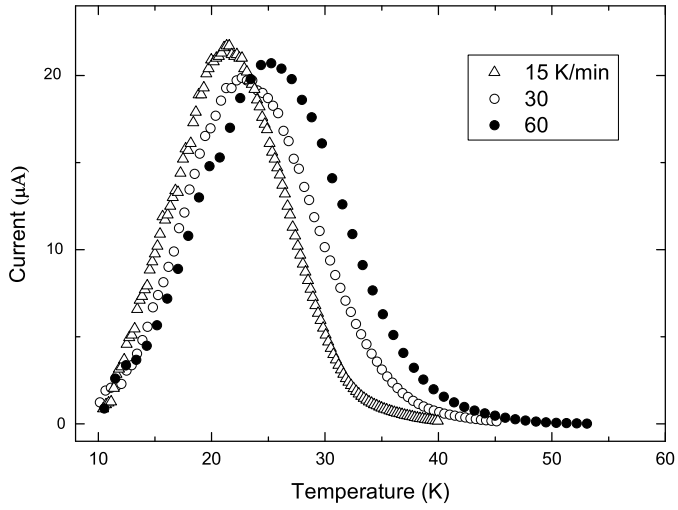

Figure 4.1: Experimental TSC spectra of $TlGaS_2$ crystal obtained with various heating rates.

heating rate. There are different methods to evaluate the trapping parameters from the experimental TSC spectra. The applicability of many of the methods is restricted if these spectra consist of a number of overlapped peaks. Here we describe the curve fitting method which we used for decomposition of the TSC spectra into separate peaks associated with the charged traps in $TlGaS_2$ crystals.

Under monomolecular conditions (i.e. slow retrapping) the TSC curve of a discrete set of traps with a trapping level E_t below the conduction band is described by the Eq. 2.20 [35].

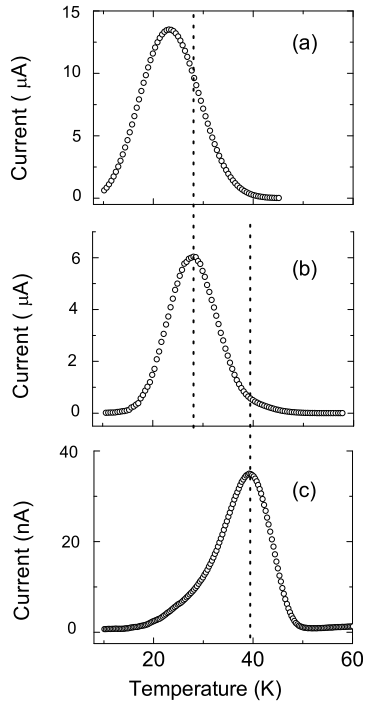

Figure 4.2: Experimental TSC spectra of $TlGaS_2$ crystal with a heating rate of 30 K/min:(a) without thermal cleaning; (b) after the first thermal cleaning at $T_1 = 22.5$ K; (c) after the second thermal cleaning at $T_2 = 28.0$ K. Vertical dotted lines show the peak positions.

In order to analyze all peaks of spectra simultaneously, the fitting function comprising the sum of all features of the TSC spectra was built as eq. 2.22.

An attempt to fit the theoretical curve using eq. 2.19 to obtained experimental data (Fig. 4.2 a) using only single peak wa not successful. This fact forced us to fit these data by means of two peaks (designated T_1 and T_2). As a result we obtained a good fit to the experimental data.

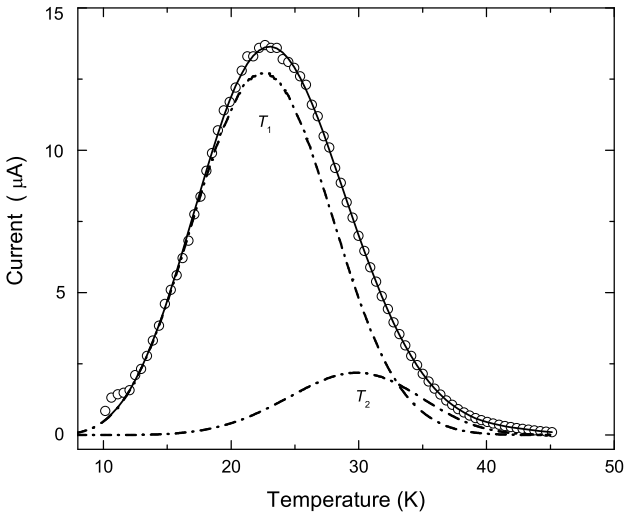

Figure 4.3: Decomposition into two separate peaks of the TSC spectrum shown in figure 4.2(a). Open circles are experimental data, the dashed curves represent decomposed peaks, and the solid curve shows the total fit to the experimental data.

Figure 4.3 shows the data for heating rate of 30 K/min fitted with two peaks with activation energies $E_{t1} = 6$ meV and $E_{t2} = 12$ meV. To verify the presence along with first peak ($T_1 = 22.5$ K) of the second peak ($T_2 = 29.9$ K) in the high-temperature side of the spectra, we decided to use so-called "thermal cleaning" procedure. Thermal cleaning procedure was applied as follows: The sample was cooled and irradiated at 10 K. The crystal was taken through the same heating cycle as before but was stopped at a temperature near T_1. In this way, the traps responsible for the current peaks for $T < T_2$ were substantially emptied. The crystal was then recooled and reheated in the dark at the same constant rates.

Figure 4.2b shows the thermally cleaned second peak for heating rates of $\beta = 30$ K/min in the $10-60$ K temperature range. The quenching of high-intensity first peak enables us to see the small details of the remaining part. Attempts to fit the theoretical curve to experimental data of thermally cleaned peak using only single peak again did not have a success. This fact are encouraged us to fit these data by means of two peaks (designated T_2 and T_3). As a result we obtained a good fit to the experimental data. Figure 4.4 shows the data fitted with two peaks (with activation energies $E_{t2} = 12$ meV and $E_{t3} = 26$ meV) for heating rate of 30 K/min. To confirm the presence along with second peak ($T_2 = 28$ K) of the third peak ($T_3 = 38.1$ K) in the high-temperature side of the TSC spectra, we decided to use second "thermal cleaning" procedure for heating rate of 30 K/min. The sample was cooled and irradiated at 10 K. The crystal was taken through the same heating cycle as before but was stopped at a temperature near T_2. In this way, the traps responsible for the current peaks for $T < T_3$ were emptied. The crystal was then recooled and reheated in the dark at the same constant rate. The absence of high intensity second peak enables us to see the small details of the remaining part of the TSC spectra (Fig. 4.2c). However, since the intensity of the second peak is too large (150 times) with respect to the third one we could not see the third peak alone. We notice on the low- temperature side of TSC spectra a weak shoulder due to the second peak. Probably, in this case we could not empty entirely the trapping levels corresponding to the second peak (T_2). With more large time of thermal cleaning we would empty also the third studied peak (T_3). Therefore, we fit the obtained TSC spectra using two peaks (T_2 and

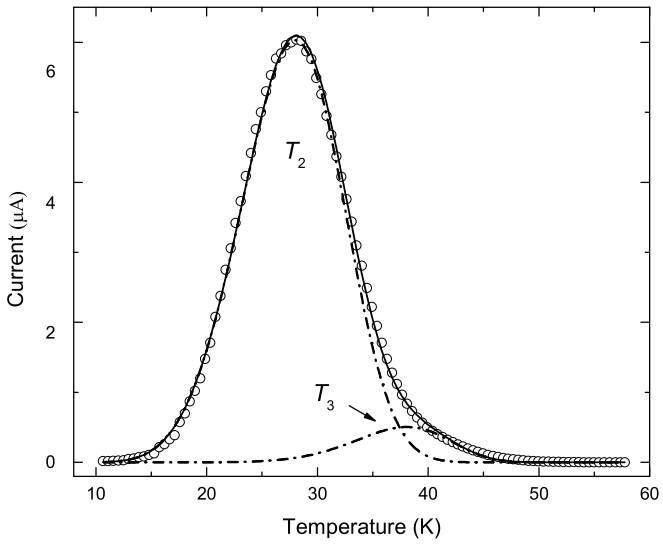

Figure 4.4: Decomposition into two separate peaks of the TSC spectrum shown in Fig. 4.2(b). Open circles are experimental data, the dashed curves represent decomposed peaks, and the solid curve shows the total fit to the experimental data.

T_3). Theoretical curves calculated for two peaks (with activation energies E_{t2} = 10 meV and E_{t3} = 26 meV) are compatible with the experimental data of the double-thermally cleaned third peak in the 10-60 K temperature range (Fig. 4.5).

Good agreement between the experimental TSC curves and theoretical ones, computed with the assumption of slow retrapping. This suggests that retrapping does not occur for the traps of $TlGaS_2$ studied in the present work. As a result, we have determined three trapping centers in $TlGaS_2$ with activation energies of 6, 13 and 25 meV (Table 4.1).

Once the curve have been fitted and the values of E_t and T_m for each peak are determined (Table 1), Eqs. 2.21 and 2.17 were used to calculate B and the attempt-to-escape frequency , ν respectively. Knowing the value of ν, one can calculate the capture cross section of the traps according to the expression

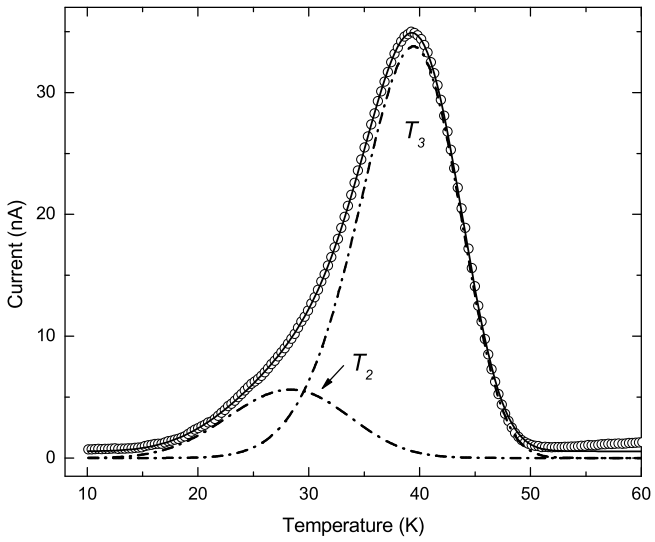

Figure 4.5: Decomposition into two separate peaks of the TSC spectrum shown in Fig. 4.2(c). Open circles are experimental data, the dashed curves represent decomposed peaks, and the solid curve shows the total fit to the experimental data.

2.23. The calculated values of S_t were found to be 1.6×10^{-23}, 2.6×10^{-22} , and 1.2×10^{-20} cm^2 for peaks T_1 , T_2 and T_3 , respectively. The small value of the capture cross sections justifies the assumption of monomolecular kinetics.

Experimental TSC curves have also been analyzed by using the peak shape method and initial rise method. In the peak shape method [37], the activation can be evaluated by using three parameters: $\tau = T_m - T_l,\ \delta = T_m - T_h,\ \omega = T_h - T_l$, where T_m is the temperature corresponding to the maximum current, T_l and T_h are the low and high half-intensity temperatures, respectively. The activation energy of the trap is determined by Eqs. 2.25-2.27.

Obtained values of μ_g for our decomposed peaks T_1, T_2 and T_3 were found to be 0.46, 0.44, and 0.43, respectively. This indicates that the retrapping process is negligible for these centers. The averaged values of activation energies E_τ, E_δ, E_ω are reported in Table 4.1. Since the peak shape method is not heating rate

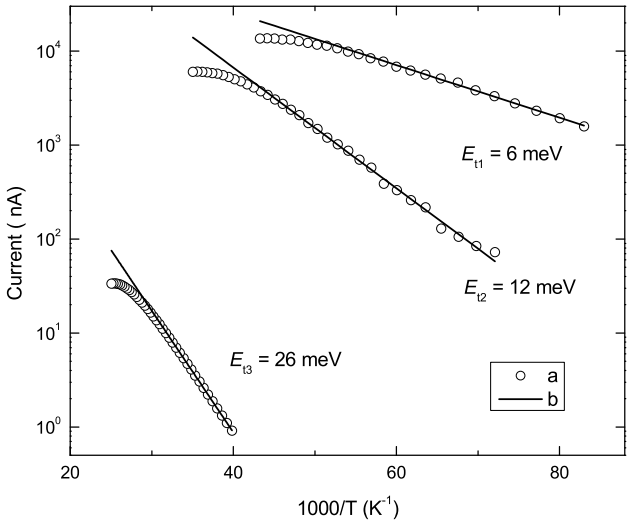

Figure 4.6: TSC versus $1000/T$ for all three peaks in the TSC spectra of $TlGaS_2$ crystal: (a) experimental data; (b) theoretical fits using the initial rise method.

Table 4.1: The activation energy E_t, the capture cross section S_t, attempt to escape frequency ν and concentration of the traps N_t in $TlGaS_2$ crystals

$Peak$	$T_m(K)$	$E_t(meV)$			$S_t(cm^2)$	$\nu(s^{-1})$	$N_t(cm^{-3})$
		Curve Fitting	*Heating Rate*	*Initial Rise*			
T_1	22.5	6	8	6	5.8×10^{-25}	9.2×10^{-1}	1.6×10^{16}
T_2	28.0	12	14	12	3.6×10^{-24}	9.1×10^{0}	5.8×10^{15}
T_3	39.4	26	22	26	3.4×10^{-23}	1.6×10^{2}	4.6×10^{13}

dependent the values of μ_g and energy values are calculated for different rates. The initial rise method [38], valid for all types of recombination kinetics, is based on the assumption that, when the traps begin to empty as the temperature is increased, the intensity of TSC is proportional to $\exp\left(-\frac{E_t}{kT}\right)$. Thus, a plot of the logarithm of the current intensity against $1/kT$ should yield a straight line with a slope of $(-E_t)$, as shown in Fig. 4.6. The progressive shift from the linear behavior at high current is due to exceeding the critical temperature T_c , after

which the exponential law is no longer valid [39]. The activation energies of the traps calculated by this procedure are found to be 20, 35 and 128 meV for peaks T_1, T_2 and T_3, respectively (Table 4.1).

4.3 Results and Discussion of the TSC Experiment of $TlGaSe_2$

Typical TSC spectra of $TlGaSe_2$ single crystals were registered at different heating rates of $\beta = 8, 11$ and 14 K/min in the $90 - 220$ K temperature range (Fig. 4.7, curves a, b and c) [41]. The TSC curves are shifted to high temperature with increase of the heating rate, as expected. We could not measure the TSC spectra in the high-temperature region ($T < 220$ K) due to strong increase of dark conductivity, which is consistent with the results reported in [1].

Our closed-cycle cryostat allowed us to perform TSC measurements in wide temperature range $10 - 300$ K. However, attempt to fill the traps at $T = 10$ K and then measure the spectra beginning from 10 K was not successful; we could not observe the TSC peaks (Fig. 4.7, curve d). Then we decided to fill the traps at higher temperatures of 20, 30, 40, 50, 60, 70, 80 K. Only filling the traps at $T = 80$ K, we were able to register the TSC peaks. This probably is associated with the presence of shallow levels acting as recombination centers in our crystal along with moderately deep traps. Indeed, in Ref. [34] the photoluminescence spectra of $TlGaSe_2$ crystal was studied and revealed out the shallow acceptor level located at $E_a = 12$ meV above the valence band. At low temperatures, electrons created by exciting light in the conduction band recombine radiatively with holes at the acceptor level of high capture cross sections. With increasing

temperature the holes are released from this level, and recombination through this channel vanishes. Above 80 K, there is only one way for the excited carriers, that is to be captured by the traps under study. In order to obtain the spectra of higher intensity we have decided to fill the traps at $T = 90$ K. There are

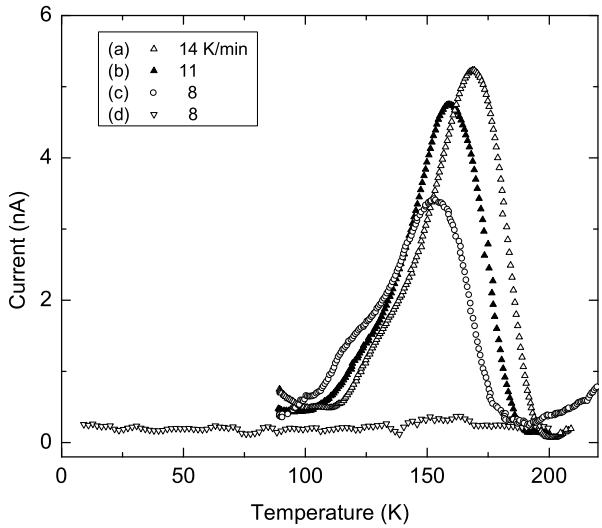

Figure 4.7: Experimental TSC spectra of $TlGaSe_2$ crystal obtained with various heating rates: 8, 11 and 14 K/min. For curves a, b and c the sample was illuminated at 90 K For curve d the illumination was performed at 10 K.

different methods to evaluate the trapping parameters from the experimental TSC spectra. The applicability of some methods are restricted if the spectra consist of a number of overlapped peaks. Here we describe the application of the curve fitting method used for decomposition of the TSC spectra into separate peaks associated with the charged traps in $TlGaSe_2$ crystals.

Attempt to fit the theoretical curve of Eqn. (2.20) to experimental data (open circles at Fig. 4.8) with only single peak was not successful. This fact forced us to fit the data by means of two peaks (designated T_1 and T_2). As a result we have obtained a good fit for the experimental data. The solid line in Fig. 4.8 shows the data for heating rate of 8 K/min fitted with two peaks with

activation energies $E_{t1} = 98$ meV and $E_{t2} = 130$ meV. The overlapping TSC peaks were also isolated by applying the "thermal cleaning" procedure [37] in order to verify the presence of T_1 and T_2 peaks. "Thermal cleaning" procedure was applied as follows: The sample was cooled and irradiated at 90 K. Then it was taken through the same heating cycle as before but was stopped at a temperature near T_1. This way, the traps responsible for the current peaks for $T < T_2$ were substantially emptied. Then, the crystal was recooled and reheated in the dark at the same rate. This allowed the observation of a sharper TSC peak at a slightly higher temperature due to electrons released from traps which are associated with the TSC maximum centered near T_2 (Fig. 4.9).

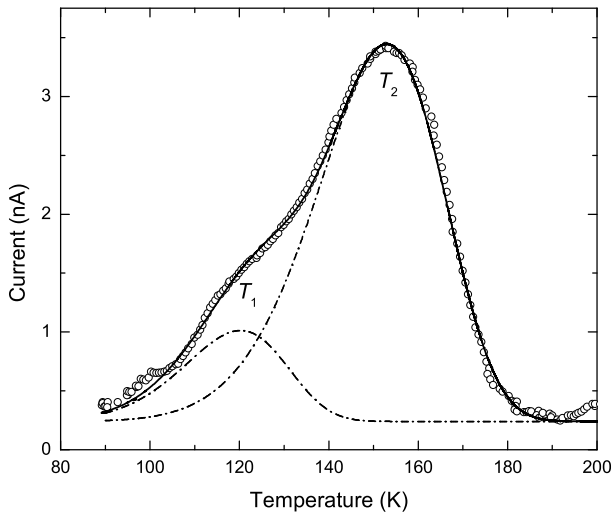

Figure 4.8: Experimental TSC spectra of $TlGaSe_2$ crystal with heating rate of 8 K/min and decomposition of this spectrum into two separate peaks. Open circles are experimental data. Dashed curves represent decomposed peaks. Solid curve shows total fit to the experimental data.

Good agreement was obtained between the experimental TSC curves and theoretical ones, computed with the assumption of slow retrapping (Fig. 4.8). This suggests that retrapping does not occur for the traps of $TlGaSe_2$ studied

in the present work. As a result, we have determined two trapping centers in $TlGaSe_2$ crystal with activation energies of 98 and 130 meV (Table 4.2). Once the curve have been fitted and the values of E_t and T_m for each peak are determined (Table 4.2), Eqns. (2.21) and (2.17) were used to calculate B and the attempt-to-escape frequency ν, respectively. Knowing the value of ν, one can calculate the capture cross section of the traps according to Eqn. (2.23) The calculated

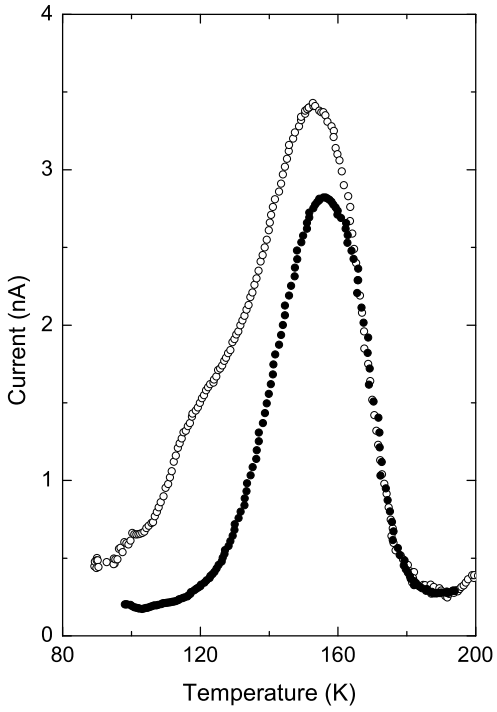

Figure 4.9: Experimental TSC spectra of $TlGaSe_2$ crystal without (open circles) and after thermal cleaning (solid circles) at $\beta = 8$ K/min.

values of S_t were found to be 2.3×10^{-24} and 1.8×10^{-24} cm^2 for peaks T_1 and T_2, respectively (Table 4.2). The small values of the capture cross section justify the assumption of monomolecular kinetics.

Experimental TSC curves have also been analyzed by using peak shape and initial rise methods. In the peak shape method [37], the activation can be evaluated by using parameters: $\tau = T_m - T_l,\ \delta = T_m - T_h,\ \omega = T_h - T_l,\ \mu_g = \delta/\omega,$

Table 4.2: The activation energy E_t, the capture cross section S_t, attempt to escape frequency ν and concentration of the traps N_t in $TlGaSe_2$ crystals

Peak	$T_m(K)$	$E_t(meV)$			$S_t(cm^2)$	$\nu(s^{-1})$	$N_t(cm^{-3})$
		Curve Fitting	*Heating Rate*	*Initial Rise*			
T_1	120.2	98	107	89	2.3×10^{-24}	1.1×10^2	1.4×10^{14}
T_2	153.0	130	142	130	1.8×10^{-24}	1.3×10^2	3.8×10^{14}

where T_m is the temperature corresponding to the maximum current, T_l and T_h are the low and high half-intensity temperatures, respectively. The activation

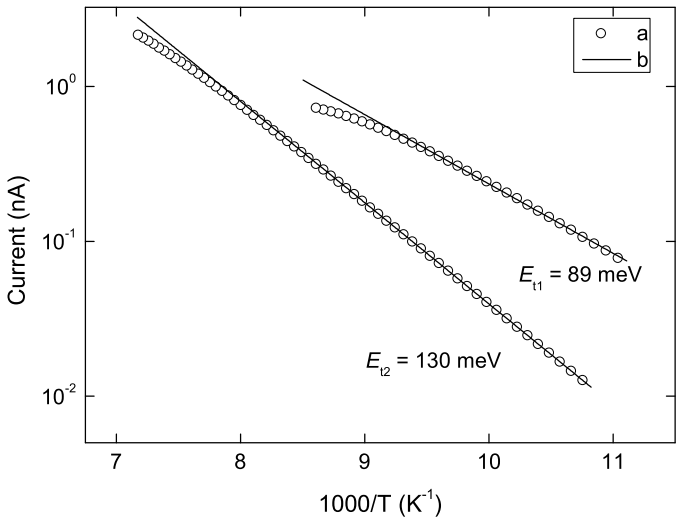

Figure 4.10: Thermally stimulated current vs. $1000/T$ for two peaks in TSC spectra of $TlGaSe_2$ crystal: (a) are experimental data; (b) are theoretical fits using initial rise method.

energy of the trap is determined by Eqs. 2.25-2.27. The values of μ_g were predicted by Chen and Kirsh [37] as 0.42 and 0.52 for the first- and second-order kinetics, respectively. Determined values of μ_g for our decomposed peaks T_1 and T_2 were found to be 0.44 and 0.45, respectively. This indicates that the retrapping process is negligible for these traps. The averaged values of obtained

activation energies E_τ, E_δ and E_ω for each peak are reported in Table 4.2.

Initial rise method [38], valid for all types of recombination kinetics, is based on the assumption that, when the traps begin to empty as temperature is increased, the TSC is proportional to $\exp(E_t/kT)$. Thus, a plot of the logarithm of the current versus 1/T should yield a straight line with a slope of $(-Et/k)$, as shown in Fig. 4.10. The progressive shift from the linear behavior at high current is due to exceeding the critical temperature T_c, after which the exponential law is no longer valid [39]. The activation energies of the traps calculated by the "initial rise method" are found to be 89 and 130 meV for peaks T_1 and T_2, respectively (Table 4.2).

4.4 Results and Discussion of the TSC Experiment of $TlInS_2$

Figure 4.11 shows typical TSC curves for $TlInS_2$ single crystal, measured at three linear heating rates of $\beta = 6, 10$ and 18 K/min in the $10-70$ K temperature range [42]. The amount of thermally stimulated current gradually increases and the maximum temperatures (T_m) shift to higher temperatures as the heating rate is increased. There are several methods in the literature to evaluate the trapping parameters from the experimental TSC spectra. We have used the curve fitting, heating rate and initial rise methods.

Good agreement has been obtained between the experimental TSC curve and theoretical one, computed with the assumption of slow retrapping (Fig. 4.12). This suggests that retrapping does not occur for the traps of $TlInS_2$ studied in the present work. As a result, we have determined trapping center in $TlInS_2$

crystal with activation energy of 12 meV (Table 4.3).

Once the curve have been fitted and the values of E_t and T_m for peak are determined (Table), Eqs. (2.21) and (2.17) were used to calculate B and the attempt-to-escape frequency ν, respectively. Knowing the value of ν, one can calculate the capture cross section of the traps according to Eqn. (2.23)

The calculated value of S_t was found to be 9.2×10^{-26} cm^2 (Table 4.3). The small value of the capture cross section justifies the assumption of monomolecular kinetics.

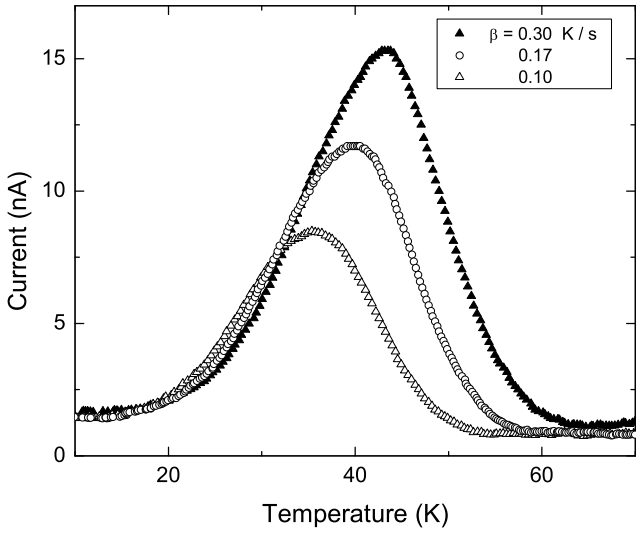

Figure 4.11: Experimental TSC curves for $TlInS_2$ crystal, measured at three linear heating rates: 6, 10 and 18 K/min.

If various heating rates are employed, and T_m are determined as a function of β, it is possible to derive the parameters α and E_t from the theoretical fit to the experimental data of $1/\beta$ vs. T_m using Eqn. (2.30) (Fig. 4.13). The results of fitting show that satisfactory fit is obtained with $E_t = 12$ meV and $\alpha = 0$, i.e., ν has no T dependency. The latter result allows us to obtain the energy value of E_t from the plot of $\ln(1/\beta)$ vs. $1/T$ (see inset of Fig. 4.13).

This plot gives a straight line consistent with a trap depth of 12 meV. Initial

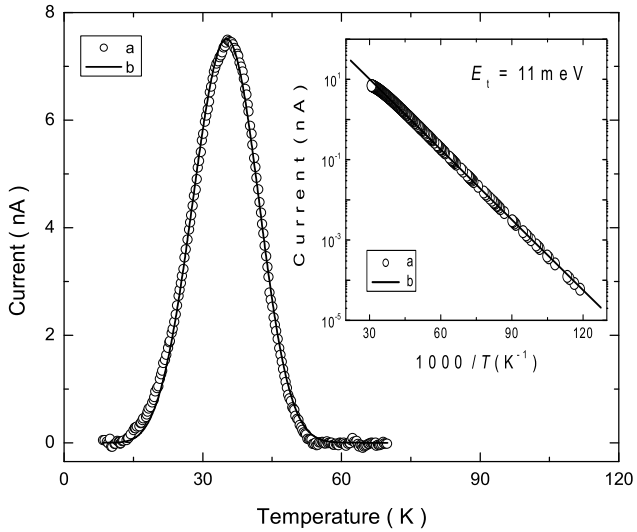

Figure 4.12: $1/\beta$ vs. T for six linear heating rates. (a) experimental data; (b) theoretical fit using equation (2.29). Inset: $\ln(1/\beta)$ vs. $1000/T$ for six different heating rates. (a) experimental data; (b) theoretical fit to the experimental data.

rise method [38], valid for all types of recombination kinetics, is based on the assumption that, when the traps are emptied with increase of temperature, the TSC is proportional to $\exp(E_t/kT)$. Thus, a plot of the logarithm of the current versus $1/T$ should yield a straight line with a slope of (E_t/k), as shown in inset of Fig. 4.12. The activation energy of the traps calculated by this procedure is found to be 11 meV (Table 4.3).

Table 4.3: The activation energy E_t, the capture cross section S_t, attempt to escape frequency ν and concentration of the traps N_t in $TlInS_2$ crystals

Peak	$T_m(K)$	$E_t(meV)$			$S_t(cm^2)$	$\nu(s^{-1})$	$N_t(cm^{-3})$
		Curve Fitting	*Heating Rate*	*Initial Rise*			
T_1	35.2	12	13	11	9.2×10^{-26}	3.9×10^{-1}	1.7×10^{14}

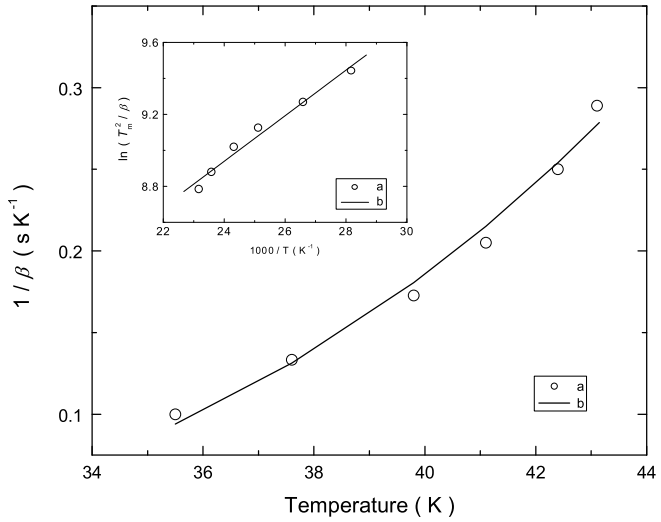

Figure 4.13: Experimental TSC spectrum of $TlInS_2$ crystal obtained with heating rate of 6 K/min. (a) experimental data; (b) theoretical fit to the experimental data. Inset: The plot of current vs. $1000/T$ for initial rise part of TSC peak. (a) experimental data; (b) theoretical fit using initial rise method.

CHAPTER 5

SUMMARY AND CONCLUSIONS

Three trapping levels at 6, 12 and 26 meV have been revealed in as-grown $TlGaS_2$ single crystals from TSC measurements. The capture cross sections of the traps were calculated to be 5.8×10^{-25}, 3.6×10^{-24} and 3.4×10^{-23} cm^2. Also, the concentration of the traps were estimated to be 1.6×10^{16}, 5.8×10^{15} and 4.6×10^{13} cm^{-3}.

Using TSC technique two trapping levels at 98 and 130 meV have been detected in as-grown $TlGaSe_2$ layered single crystals by the TSC technique. The capture cross section of the traps were found to be 2.3×10^{-24} and 1.8×10^{-24} cm^2. The concentration of the traps were evaluated as 1.4×10^{14} and 3.8×10^{14} cm^{-3}.

A trapping level at 12 meV has been detected in as-grown $TlInS_2$ layered single crystals by TSC technique. The capture cross section of the traps was calculated to be 9.2×10^{-26} cm^2. The concentration of the traps was estimated to be 1.7×10^{14} cm^{-3}.

Thus, three, two and one trapping levels have been detected by the TSC technique in as-grown $TlGaS_2$, $TlGaSe_2$ and $TlInS_2$ layered crystals, respectively. Since studied crystals are not intentionally doped, the observed trap levels are thought to originate from defects, created during the growth of crystals, and/or

unintentional impurities. The trap parameters were determined by various methods of analysis, and they agree well with each other. The retrapping process is negligible for these levels, as confirmed by the good agreement between the experimental results and the theoretical predictions of the model that assumes slow retrapping. The activation energy, capture cross section, attempt-to-escape frequency and concentration of the traps in $TlGaS_2$, $TlGaSe_2$ and $TlInS_2$ crystals were determined. Also, the ability of TSC to perform a quantitative analysis of shallow levels in *p*-type $TlGaS_2$, $TlGaSe_2$ and $TlInS_2$ layered crystals has been demonstrated.

REFERENCES

[1] M. P. Hanias, A. N. Anagnostopoulos, K. Kambas, J. Spyridelis, Mater. Res. Bull. **27**, (1992) 25.

[2] S. G. Abdullaeva, G. L. Belenkii, N.T. Mamedov, Sov. Phys. Semicond. **15**, (1981) 540.

[3] J. A. Kalomiros, N. Kalkan, M. Hanias, A.N. Anagnostopoulos, K. Kambas, Solid State Commun. **96**, (1995) 601.

[4] K. A. Yee, A. Albright, J. Am. Chem. Soc., **113**, (1991) 6474 (and references therein).

[5] A. E. Bakhyshov, A. A. Lebedev, Z.D. Khalafov, M.A. Yakobson, Sov. Phys. Semicond., **12**, (1978) 320.

[6] K. R. Allakhverdiev, Solid State Commun. **111**, (1999) 253.

[7] N. Kalkan, J. A. Kalomiros, M. Hanias, A.N. Anagnostopoulos, Solid State Commun. **99**, (1996) 375.

[8] H. J. Song, S. H. Yun, W.T. Kim, Solid State Commun. **94**, (1995) 225.

[9] N. M. Gasanly, A. Aydinli, A. Bek, I. Yilmaz, Solid State Commun. **105**, (1998) 21.

[10] G. Micocci, A. Serra, A. Teporre, J. Appl. Phys. **81**, (1997) 6200.

[11] E. Borchi, M. Bruzzi, S. Pirollo, S. Sciortino, J. Phys. D: Appl. Phys. **31**, (1998) L93.

[12] E. Hernandez, L. Duran, C.A. Durante Rincon, G. Aranguren, C.Guerrero, J. Naranjo, Cryst. Res. Technol. **37**, (2002) 1227.

[13] W. Henkel, H.D. Hochheimer, C. Carlone, A. Werner, S. Ves, H.G. von Schnering, Phys. Rev. B **26**, (1982) 3211.

[14] G. B. Abdullaev, K. R. Allakhverdiev, R. Kh. Nani, E. Yu. Salaev, R. M. Sardarly, Phys. Status Solidi (a) **34**, (1976) K115.

[15] N. M. Gasanly, B. G. Akinoglu, S. Ellialtioglu, R. Laiho, A. E. Bakhyshov, Physica B **192**, (1993) 371.

[16] C. S. Yoon, B. H. Kim, D. J. Cha W. T. Kim, Japan J. Appl. Phys. **32**, (1993) 555.

[17] G. I. Abutalybov, I. Kh. Akopyan, I.K. Neimanzade, B. V. Novikov E.Yu. Salaev, Sov. Phys. Solid State **27**, (1985) 1710.

[18] S. G. Abdullaeva, N. T. Mamedov, Sov. Phys. Solid State **28**, (1986), 499.

[19] C. S. Yoon, S. J. Chung, S.J. Nam, W.T. Kim, Cryst. Res. Technol. **31**, (1996) 229.

[20] A. E. Bakhyshov, B. A. Natig, B. Safuat, S. R. Samedov, Sh. M. Abbasov, Sov. Phsy. Semicond. **27**, (1990) 828.

[21] J. . Kalomiros, A.N. Anagnostopoulos, Phys. Rev. B **50**, (1994) 7488.

[22] K. R. Allakhverdiev, T. G. Mammadov, R.A Suleymanov, N. Z. Gasanov, J. Phys.: Condens. Matter **2**, (2003) 1291

[23] N. Kalkan, D. Papadopoulos, A. N. Anagnostopoulos , J. Spydelis, Mat. Res. Bull. **28**, (1993) 693.

[24] N. M. Gasanly, H. Ozkan, M. Tas, Cryst. Res. Technol. **35**, (2000) 185.

[25] M. P. Hanias, A.N. Anagnostopoulos, K. Kambas, J. Spyridelis, Physica B **160**, (1989) 154.

[26] A. F. Qasrawi, N.M. Gasanly, Phys. Stat. Solidi A **199**, (2003) 277.

[27] N. Kalkan, M.P. Hanias, A.N. Anagnostopoulos, Mat. Res. Bull. **27**,(1992) 1329.

[28] N. S. Yuksek, N.M. Gasanly, A. Aydinli, J. Raman Spectroscopy **35**, (2004).

[29] A. Aydinli, N.M. Gasanly, I. Yilmaz, A. Serpenguzel, Semicond. Sci. Technol. **14**, (1999) 599.

[30] S. Ozdemir, R.A. Suleymanov, E. Civan, T. Firat, Solid State Commun. **98**, (1996) 385.

[31] B. G. Markey, Deep Level Characterization of Seeded Physical Vapor Transport Zinc Selenide (PhD Thesis, Oklahoma, 1993).

[32] A. Halperin, A. A. Braner, Phys. Rev. **117**, (1960) 408.

[33] H. F. Wilkins, Proc. Roy. Soc. (London)**A184**, (1945) 366.

[34] N. M. Gasanly, A. Serpenguzel, A. Aydinli, S. M. A. Baten, J. Lumin. **86**, (2000) 39.

[35] T. A. T. Cowell, J. Woods, Brit. J. Appl. Phys. **18**, (1967)1045.

[36] N. S. Yuksek, N. M. Gasanly, H. Ozkan, Semicond. Sci. Technol. **18**, (2003) 834.

[37] R. Chen, Y. Kirsh, *Analysis of Thermally Stimulated Processes*, Pergamon Press, Oxford, 1981, p. 275.

[38] K. H. Nicholas, J. Woods, Brit. J. Appl. Phys. **15**, (1964) 783.

[39] G. Micocci, A. Rizzo, A. Tepore, J. Appl. Phys. **54**, (1983) 1924.

[40] C. Manfredotti, R. Murri, A. Quirini, L. Vasanelli, Phys. Status Solidi (a) **38**, (1976) 685.

[41] N. S. Yuksek, H. Kavas, N. M. Gasanly, H. Ozkan, Physica B **344**, (2004) 249.

[42] N. S. Yuksek, N. M. Gasanly, H. Ozkan, O. Karci, Acta Physica Pol. A **106**, (2004) ....